COMPARATIVE STUDY ON WEAR PERFORMANCE OF TRADITIONAL AND NANOSTRUCTURED Al_2O_3–13 wt. % TiO_2 AIR PLASMA SPRAY COATINGS

SUN-HUI YAO

Bachelor Degree Program in Technology Management, Chang Jung Christian University, Kway Jen, Tainan 71101, Taiwan

E-mail: shyao0954@gmail.com

Submitted November 11, 2014; accepted March 18, 2015

Keywords: Nanostructured materials, Wear, Air Plasma Spray, Al_2O_3, TiO_2

This study is an attempt to understand the difference between traditional and nanostructured Al_2O_3 – 13 wt. % TiO_2 air plasma spray (APS) coatings. Both coatings were prepared using commercial feedstock powders. The resulting coatings were comparatively studied by means of the micro Vickers hardness tester, XRD, SEM, EDX and SRV® reciprocating sliding wear tester. The results showed that remarkable deviations were found between these two coatings. Compared with the traditional coating as a reference, the nanostructured coating showed hardness enhancement (Hv998 vs. Hv895) and wear improvement reaching 60 %. The mechanisms involved were discussed.

INTRODUCTION

Al_2O_3 ceramics, because of high hardness and thermal stability nature, have been widely used in severe conditions, such as heavy wear and corrosion combined with high temperature. Al_2O_3 ceramics are also the basis of the most generally used thermal barrier materials [1-3]. To improve the inevitable brittleness while retaining high hardness, a mixture with a certain small amount of TiO_2 is favorable, i.e. Al_2O_3–13 wt. % TiO_2. Yugeswaran et al. [4] studied the effect of TiO_2 content on Al_2O_3–TiO_2 coatings; they concluded that hardness and porosity changed with the TiO_2 content.

Researchers have found that nanostructured materials have totally different properties from traditional (micro-scale) materials, for example, ultra-high hardness, toughness or excellent wear resistance. The significantly increased performance results from the fact that the huge amounts of borders, which exist in nanostructured materials, hinder/deflect the growth of cracks effectively [5-6]. Tian et al. [1] and Song et al. [7] studied nanostructured Al_2O_3–TiO_2 coatings and found that they showed better performance in hardness, wear, corrosion and thermal shock tests than traditional coatings with identical composition.

In this work, two kinds of Al_2O_3−13 wt. %TiO_2 air plasma spray (APS) coatings were synthesized using commercial nanostructured and traditional Al_2O_3––13 wt. % TiO_2 powders, with the aim to explore the nanostructure effects on these properties evaluated.

EXPERIMENTAL

Three kinds of commercial feedstock powders were used, i.e. traditional Al_2O_3–13 wt. % TiO_2 (130SF, Sulzer Metco), nanostructured Al_2O_3–13 wt. % TiO_2 (NanoxS2613S, Inframat Advanced Materials) and Ni−5 wt. % Al powder (450NS, Sulzer Metco). The nominal composition of the traditional powder is 13 wt. % TiO_2 and 87 wt. % Al_2O_3, while that of the nanostructured powder is 11 wt. % TiO_2, 8 − 10 wt. % ZrO_2, 6 − 8 wt. % CeO_2, the balance being Al_2O_3.

The specimen substrates were JIS S31C steel and with a dimension of 24 mm in diameter and 7.9 mm in thickness. The coatings were produced using a Sulzer Metco 9MB gun on a 9MC semi-automatic plasma spray system. Prior to coating, the substrates were grit blasted to obtain a surface roughness Ra ~ 10 μm, pre-heated to 200°C for 60 sec, and then a bond coating of Ni−5 wt. % Al was deposited.

The spraying parameters, which had been optimized based on bending tests, were as follows: first, for the Ni−5 wt. % Al bond coating - primary gas Ar 90 SCFH, secondary gas H_2 15 SCFH, carrier gas Ar 13.5 SCFH, current 500 A, voltage 64 - 70 V, powder feed rate 50 g min^{-1}, spray distance 5.5 in (0.140 m), thickness 100 ± 20 μm; second, for the Al_2O_3–TiO_2 top coating – primary gas Ar 90 SCFH, secondary gas H_2 15 SCFH, carrier gas Ar 13.5 SCFH, current 500 A, voltage 64 - 70 V,powder feed rate 40 g min^{-1}, spray distance 3.0 in (0.076 m), thickness 300 ± 50 μm.

The cross-sectional microstructure and worn conditions of coatings were examined using an SEM (Hitachi SU8000, Japan) equipped with an EDX (QUANTAX Bruker, Germany). XRD analyses (D/MAX-2500, Regaku, Japan) were conducted using grazing angle diffraction with an X-ray incident angle of 2°. The micro Vickers hardness tester (HMV-2, Shimadzu, Japan) was operated at an applied load 200 g for 15 s.

An SRV® reciprocating sliding wear system (Schwingung Reibung and Verschleiss tester, Optimal Instruments Prüftechnik GmbH, Germany) was used to evaluate the wear performance employing a ball-on-disk point-contact mode [8]. The counterparts employed alumina balls. The following experimental parameters were used: no lubricant, applied load 10 N, stroke 0.5 mm, frequency 30 Hz and duration 60 min. The wear scar was measured for the maximal wear depth by using a surface profilometer (SE30H, Kosaka, Japan).

RESULTS AND DISCUSSION

Figures 1 and 2 show the micrographs of traditional and nanostructured Al_2O_3–13 wt. % TiO_2 powders, respectively. The traditional Al_2O_3–13 wt. % TiO_2 powder consisted of a micro-sized Al_2O_3 particle clad with nano-sized TiO_2 particles. Due to fusing and crushing, the Al_2O_3 particles showed angular and blocky morphology, as shown in Figure 1. The traditional Al_2O_3–13 wt. % TiO_2 powder was with 10 - 45 μm in three dimensions. The nanostructured Al_2O_3–13 wt. % TiO_2 powder, showing a spheroidal contour (Figure 2a), was an agglomeration of nanosized Al_2O_3 and TiO_2, as shown in Figure 2b. The nanostructured Al_2O_3–13 wt. % TiO_2 powder was with 5 - 30 μm in diameter.

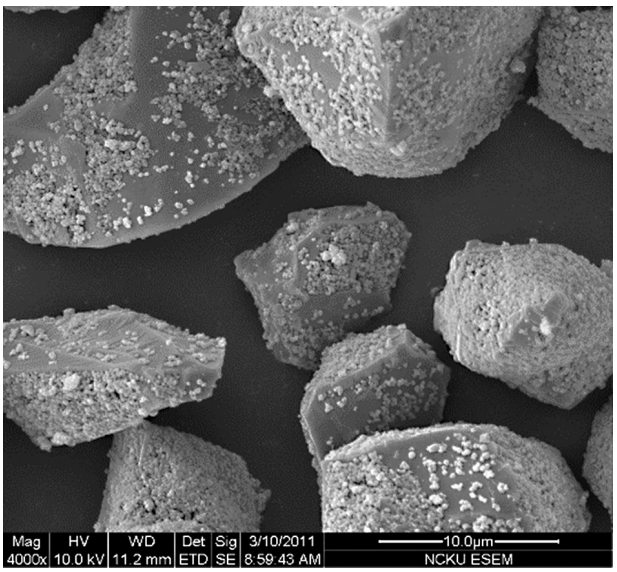

Figure 1. SEM micrograph of traditional Al_2O_3–13 wt. % TiO_2 powder.

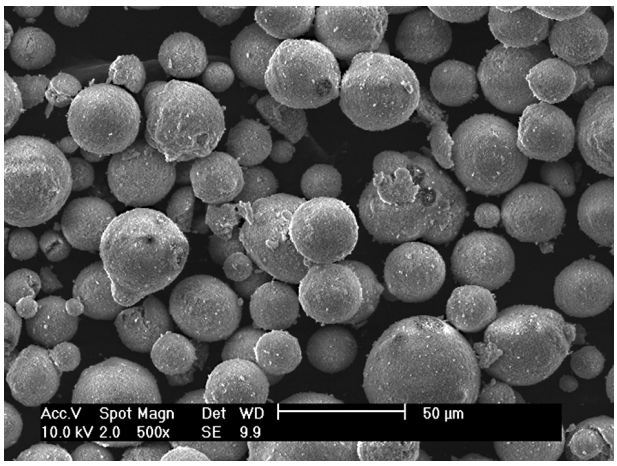

a)

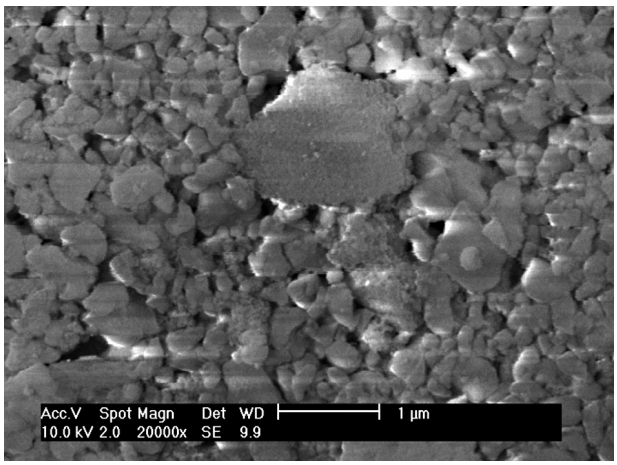

b)

Figure 2. SEM micrograph of: a) nanostructured Al_2O_3–13 wt. % TiO_2 powder and b) cross-sectional microstructure of a powder.

Figures 3 and 4 show SEM micrographs of cross-sectional microstructure of traditional and nanostructured coatings, respectively. As can be seen, the nanostructured coating (Figure 4a) shows less porosity than the traditional one (Figure 3a). Figure 3b shows the back scatter electron (BSE) image of Figure 3a, in which the bright layers are TiO_2 phase, while the dark layers are Al_2O_3 phase. In contrast to the thicker and less homogeneous TiO_2 layers within the traditional coating (Figure 3b), the TiO_2 layers within the nanostructured coating could hardly be identified (Figure 4b).

Figure 5 shows the XRD of patterns of traditional and nanostructured Al_2O_3–13 wt. % TiO_2 powders; both were of nearly identical constituent phases, containing a major α-Al_2O_3 phase and a minor anatase-TiO_2 phase. The ZrO_2 and CeO_2 phases were used as a stabilizer for the nanostructured powder, as shown in Figure 5b.

Figure 6 shows the XRD patterns of traditional and nanostructured Al_2O_3–13 wt. % TiO_2 coatings. These two patterns reveal some common points: the coatings were composed of an unstable γ-Al_2O_3 phase

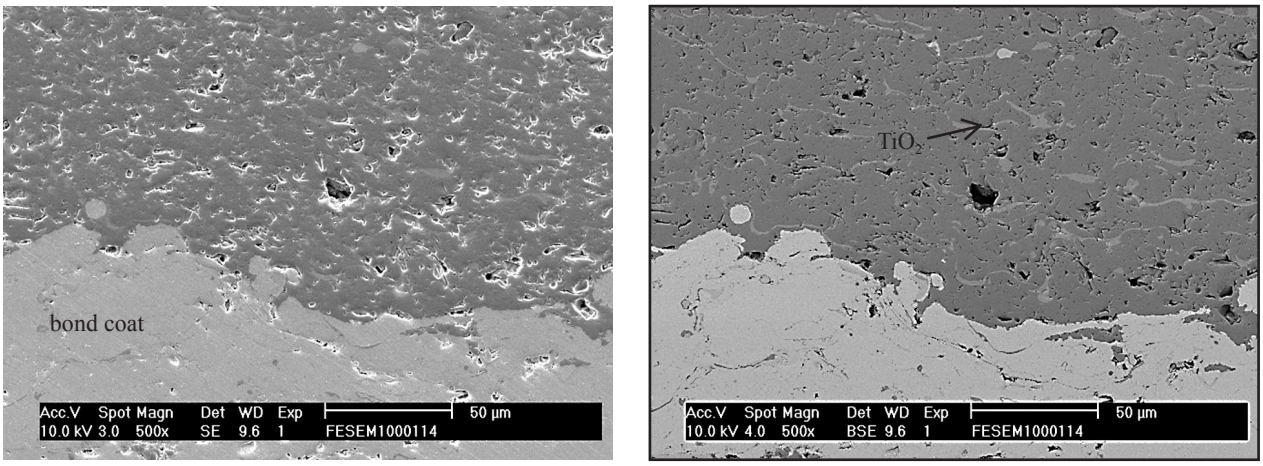

a) SEM micrograph b) BSE image

Figure 3. SEM micrograph of traditional Al_2O_3–13 wt. % TiO_2 coating; b) BSE image of (a).

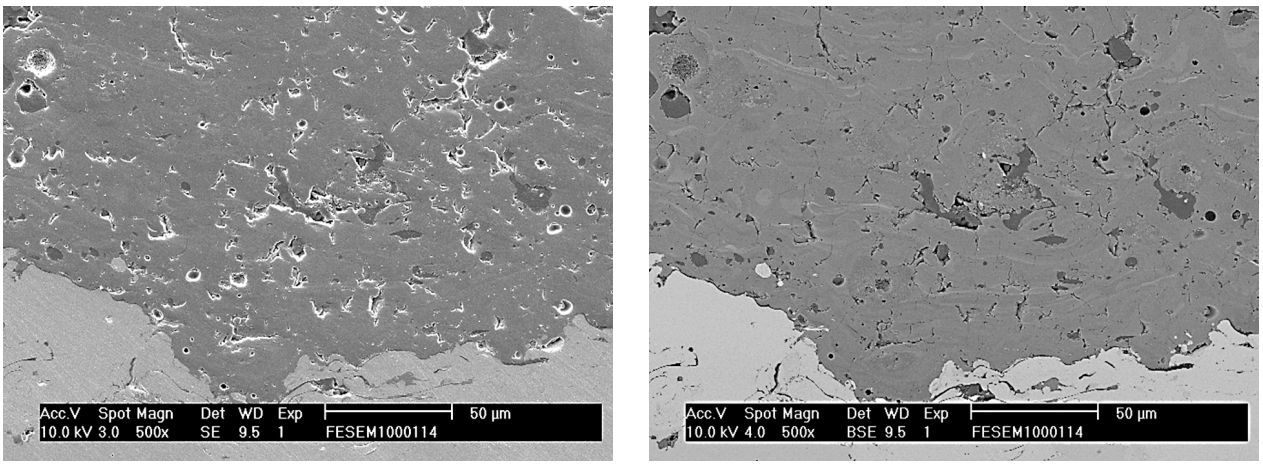

a) SEM micrograph b) BSE image

Figure 4. SEM micrograph of nanostructured Al_2O_3–13 wt. % TiO_2 coating; b) BSE image of (a).

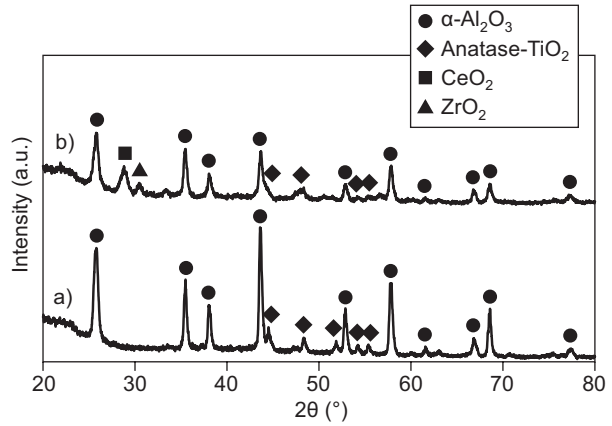

Figure 5. XRD patterns of Al_2O_3–13 wt. % TiO_2 powders: a) traditional and b) nanostructured.

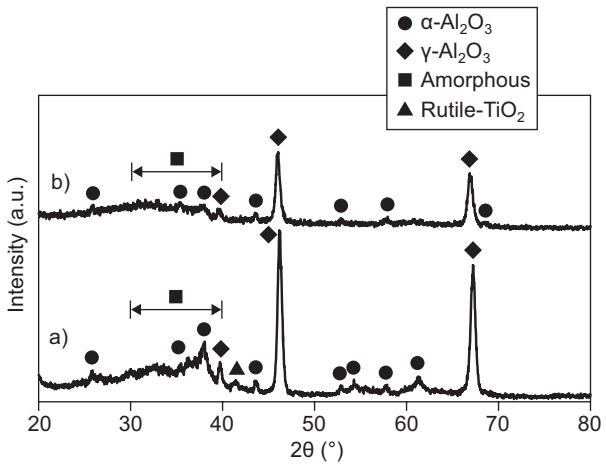

Figure 6. XRD patterns of Al_2O_3–13 wt. % TiO_2 coatings: a) traditional and b) nanostructured.

with a minor stable α-Al_2O_3 phase and an amorphous phase (2θ = 25 ~ 40°). The transformation of α-Al_2O_3 phase to γ-Al_2O_3 phase and the amorphous phase resulted from the rapid heating and cooling process when powders flew through high temperature plasma atmosphere [9]. However, since each nanostructured powder was an agglomeration of nanosized fragments (Figure 1b), the resulting nanostructured coating showed certain extent of distinction, which can be explained using the small mass effect of nanostructured materials. In Figure 6, one can see that the nanostructured coating shows a higher degree of amorphization than the traditional coating. In addition, although the patterns indicate that both coatings consisted of γ-Al_2O_3 phase and a small amount of α-Al_2O_3 phase, the mechanisms involved were completely different. For the traditional coating, its raw material (powder) comprised microsized α-Al_2O_3 particles clad with nanosized TiO_2 fragments, as shown in Figure 1. When the traditional powders flew through plasma atmosphere of extremely high temperature, part of each powder experienced drastic melting and then rapid cooling, which made the α-Al_2O_3 phase be transformed to the γ-Al_2O_3 phase. The unmelted part remained as α-Al_2O_3 phase. The nanosized TiO_2 fragments melted completely and transformed from anatase-TiO_2 (Figure 5a) to rutile-TiO_2 (Figure 6a). In comparison, when the nano-structured powders flew through plasma, most nanosized fragments, including Al_2O_3 and TiO_2, melted completely. When cooled down, the melted fragments solidified and then transformed to γ-Al_2O_3 phase with TiO_2 dissolved in it. The unmelted fragments retained their shape and nano-scale dimension. Accordingly, partially melted zones formed that consisted of the γ-Al_2O_3 phase supersaturated with Ti^{4+} as the matrix embedded in the α-Al_2O_3 phase [10]. A typical microstructure is shown in Figure 7. This result is consistent with some other similar studies [1, 11-12].

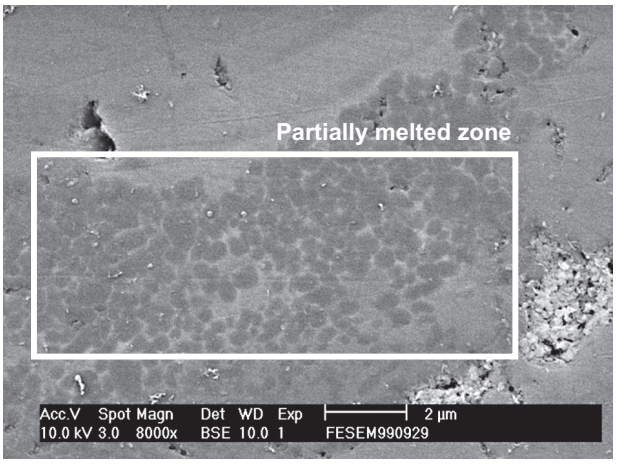

Figure 7. BSE micrograph of Al_2O_3–13 wt. % TiO_2 nanostructured coating, showing α-Al_2O_3 embedded within γ-Al_2O_3 matrix.

Tian *et al.* [1] found that the partially melted zone showed higher hardness and elastic modulus than the fully melted zone. The γ-Al_2O_3 phase shows lower hardness and higher toughness than the α-Al_2O_3 phase, and of all the Al_2O_3 phases, α-Al_2O_3 phase is the one with the highest hardness [13]. Thus, for the partially melted zone, the α-Al_2O_3 particles played a role as reinforcement for the γ-Al_2O_3 matrix. In this study, the hardness of nanostructured coating ($HV_{0.2}$ 998) was higher than the traditional one ($HV_{0.2}$ 895) by HV $100_{0.2}$. The denser microstructure (Figure 4) combined with the partially melted zone might be the major contribution to hardness enhancement for the nanostructured coating.

In the wear test, the nanostructured coating showed much better wear resistance (1.10 vs. 2.80, μm) and lower friction coefficient (0.088 vs. 0.101) than the traditional coating. It is notable that the wear depth of nanostructured coating was less than one half of that of the traditional coating. The wear damage of counterpart was also milder for the nanostructured coating wear pair (1360 vs. 1740 μm^2).

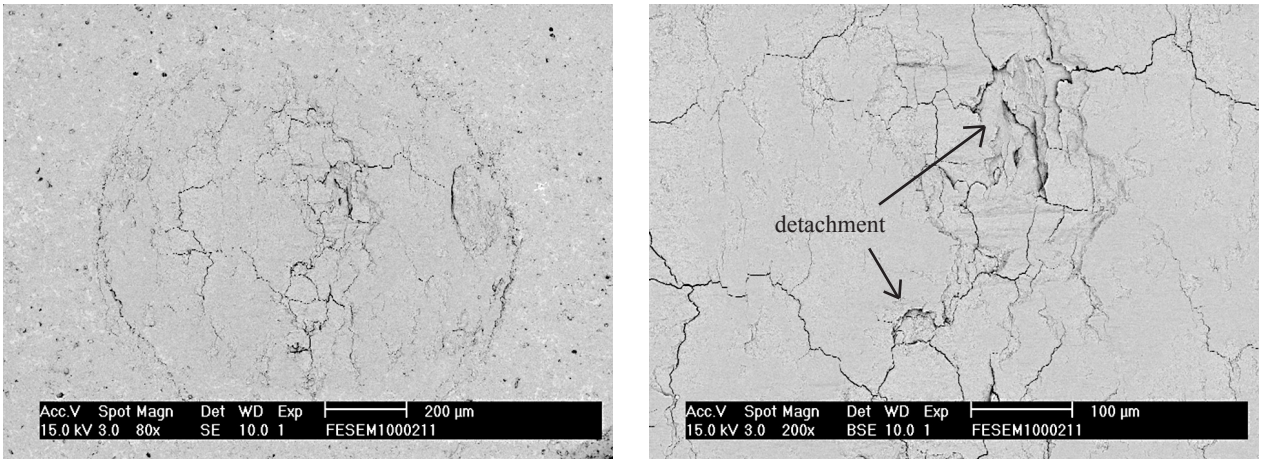

a) SEM micrograph b) magnified image

Figure 8. SEM micrograph of wear morphology of traditional Al_2O_3–13 wt. % TiO_2 coating; b) magnified image of (a).

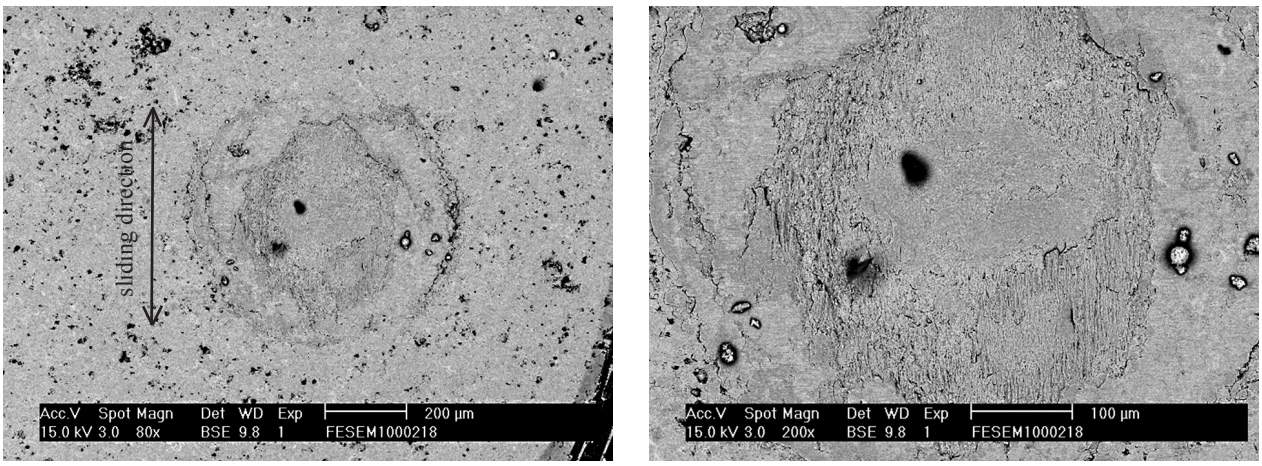

a) SEM micrograph b) magnified image

Figure 8. SEM micrograph of wear morphology of nanostructured Al_2O_3–13 wt. % TiO_2 coating; b) magnified image of (a).

Figures 8 and 9 show SEM micrographs of worn surface of traditional and nanostructured coatings, respectively. In Figure 8, one can see that many cracks formed on the wear area. As sliding continued, the cracks developed and coalesced, and then the coating was damaged by small flakes as indicated by the arrows in Figure 8b. In Comparison, in Figure 9, the plastic flow of coating material along the sliding direction dominated on the worn surface of the nanostructured coating with very few tiny cracks (Figure 9b). It is believed that the presence of partially melted areas as well as the denser structure accounted for the improved wear resistance and change in the wear mechanism. When cracks developed and grew into the partial melted areas, the α-Al_2O_3 hard particles hindered and deflected the propagating direction of cracks, and then largely reduced their growth rate, leading to a decrease of the crack intensity.

In spite of nanostructured feedstock powders having been commercialized for years, their applications are still very limited due to their relatively high cost. However, from the results of the present study, the employment of nanosized powders could be seriously considered because of higher hardness, lower friction coefficient, and far better wear resistance.

CONCLUSION

In this work, traditional and nanostructured Al_2O_3-13 wt. % TiO_2 air plasma spray coatings were prepared and compared. The nanostructured coating exhibited a denser and more homogeneous microstructure, and a distinguishing characteristic – the partially melted zone. All of these features contributed to the enhanced hardness. It is believed that the lower friction coefficient and much lower wear of nanostructured coating resulted from its higher hardness and the partially melted zone. Nanostructured Al_2O_3–TiO_2 coatings maybe considered to be good substitutes for the traditional ones due to their extraordinarily good wear performance.

REFERENCES

1. Tian W., Wang Y., Yang Y., Li C.: Surf. Coat. Tech. *204*, 642 (2009).
2. Yılmaz R., Kurt A.O., Demir A., Tatlı Z.: J. Eur.Cer.Soc. *27*, 1319 (2007).
3. Guessasma S., Bounazef M., Nardin P., Sahraoui T.: Cer. Inter. *32*, 13 (2006).
4. Yugeswaran S., Selvarajan V., Vijay M., Ananthapadmanabhan P.V., Sreekumar K.P.: Cer. Inter. *36*, 141 (2010).
5. Rodriguez J., Rico A., Otero E., Rainforth W.M.: Acta Materialia *57*, 3148 (2009).
6. Wang Y., Tian W., Yang Y.: Surf. Coat. Tech. *201*, 7746 (2007).
7. Song E.P., Ahn J.H., Lee S.H., Kim N. J.: Surf. Coat. Tech. *202*, 3625 (2008).
8. Yao S.H., Su Y.L., Kao W.H., Cheng K.W.: Surf. Coat. Tech. *201*, 2520 (2006).
9. Shaw L., Goberman D., Ren R., Gell M., Jiang S., Wang Y., Xiao T. D., Strutt P.R.: Surf. Coat. Tech. *130*, 1 (2000).
10. Gell M., Jordan E.H., Sohn Y.H., Goberman D., Shaw L., T Xiao. D, Surf. Coat. Tech. *146-147*, 48 (2001).
11. Goberman D., Sohn Y. H., Shaw L., Jordan E., Gell M.: Acta Materialia *50*, 1141 (2002).
12. Luo H., Goberman D., Shaw L, Gell M.: Mat. Sci. Eng. A *346*, 237 (2003).
13. Ouyang J.H., Sasaki S.: Tribo. Inter. 38, 49 (2005)